BIOCHEMISTRY
including biophysical chemistry & molecular biology

Accelerated Publication

pubs.acs.org/biochemistry

New Role for the Ankyrin Repeat Revealed by a Study of the *N*-Formyltransferase from *Providencia alcalifaciens*

Colin R. Woodford, James B. Thoden, and Hazel M. Holden*

Department of Biochemistry, University of Wisconsin, Madison, Wisconsin 53706, United States

Supporting Information

ABSTRACT: *N*-Formylated sugars such as 3,6-dideoxy-3-formamido-D-glucose (Qui3NFo) have been observed on the lipopolysaccharides of various pathogenic bacteria, including *Providencia alcalifaciens*, a known cause of gastroenteritis. These unusual carbohydrates are synthesized *in vivo* as dTDP-linked sugars. The biosynthetic pathway for the production of dTDP-Qui3NFo requires five enzymes with the last step catalyzed by an *N*-formyltransferase that utilizes N^{10}-tetrahydrofolate as a cofactor. Here we describe a structural and functional investigation of the *P. alcalifaciens N*-formyltransferase, hereafter referred to as QdtF. For this analysis, the structure of the dimeric enzyme was determined in the presence of N^5-formyltetrahydrofolate, a stable cofactor, and dTDP-3,6-dideoxy-3-amino-D-glucose (dTDP-Qui3N) to 1.5 Å resolution. The overall fold of the subunit consists of three regions with the N-terminal and middle motifs followed by an ankyrin repeat domain. Whereas the ankyrin repeat is a common eukaryotic motif involved in protein−protein interactions, reports of its presence in prokaryotic enzymes have been limited. Unexpectedly, this ankyrin repeat houses a second binding pocket for dTDP-Qui3N, which is characterized by extensive interactions between the protein and the ligand. To address the effects of this second binding site on catalysis, a site-directed mutant protein, W305A, was constructed. Kinetic analyses demonstrated that the catalytic activity of the W305A variant was reduced by approximately 7-fold. The structure of the W305A mutant protein in complex with N^5-formyltetrahydrofolate and dTDP-Qui3N was subsequently determined to 1.5 Å resolution. The electron density map clearly showed that ligand binding had been completely abolished in the auxiliary pocket. The wild-type enzyme was also tested for activity against dTDP-3,6-dideoxy-3-amino-D-galactose (dTDP-Fuc3N) as a substrate. Strikingly, sigmoidal kinetics indicating homotropic allosteric behavior were observed. Although the identity of the ligand that regulates QdtF activity *in vivo* is at present unknown, our results still provide the first example of an ankyrin repeat functioning in small molecule binding.

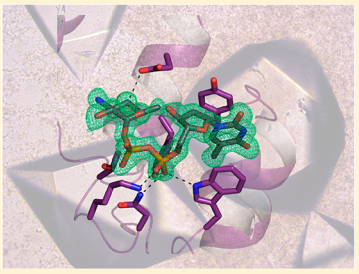

The lipopolysaccharide or LPS is a complex glycoconjugate associated with the outer membranes of Gram-negative bacteria where it provides a permeability barrier to hydrophobic or negatively charged molecules.[1] It can be envisioned in terms of three specific components: lipid A, the core oligosaccharide, and the O-specific polysaccharide or O-antigen. It is the O-antigen, which extends farthest from the bacterium, that contributes to the wide species variations seen in nature. Quite unusual dideoxysugars are often found on the O-antigens of pathogenic Gram-negative bacteria, including 3,6-dideoxy-3-formamido-D-glucose (Qui3NFo) or 3,6-dideoxy-3-formamido-D-galactose (Fuc3NFo), which are shown in Scheme 1a. The first step in the biosynthetic pathway for the production of Qui3NFo in bacteria involves the attachment of a dTMP moiety to glucose 1-phosphate to yield dTDP-glucose. This step is followed by a 4,6-dehydration, a 3,4-ketoisomerization, and an amination reaction. The last step in the biosynthetic pathway is catalyzed by an *N*-formyltransferase, which requires N^{10}-formyltetrahydrofolate for activity (Scheme 1b).

Herein, we report a structural and functional investigation of the *N*-formyltransferase from *Providencia alcalifaciens*, a pathogenic organism linked to the 1996 food poisoning outbreak in Japan.[2] The high-resolution structures of the enzyme, hereafter referred to as QdtF, were determined in the presence of N^5-formyltetrahydrofolate [a stable analogue (Scheme 1c)] and dTDP-sugar substrates. Strikingly, the N-terminal catalytic region of the enzyme is followed by ankyrin repeats. The occurrence of such repeats in QdtF is highly unusual as they are typically found in eukaryotic proteins. First identified in the *Drosophila* signaling protein Notch and in the yeast cell cycle regulator Swi6/Cdc10, the ankyrin repeat is now known to be one of the most commonly occurring molecular architectures in eukaryotic proteins involved in processes such as the cell cycle, transcriptional regulation, signal transduction, and modulation of the inflammatory response.[3−6]

Remarkably, the ankyrin repeat domain in QdtF harbors a second binding pocket for the dTDP-sugar substrate that is characterized by extensive interactions between the ligand and protein side chains. To the best of our knowledge, ankyrin repeats have never been implicated in small molecule binding. Taken together, the molecular and biochemical data from our investigation expand the repertoire of ankyrin repeats from protein−protein interactions to small molecule binding and allosteric control.

Received: December 18, 2014
Revised: January 9, 2015
Published: January 9, 2015

DOI: 10.1021/bi501539a
Biochemistry 2015, 54, 631−638

Scheme 1

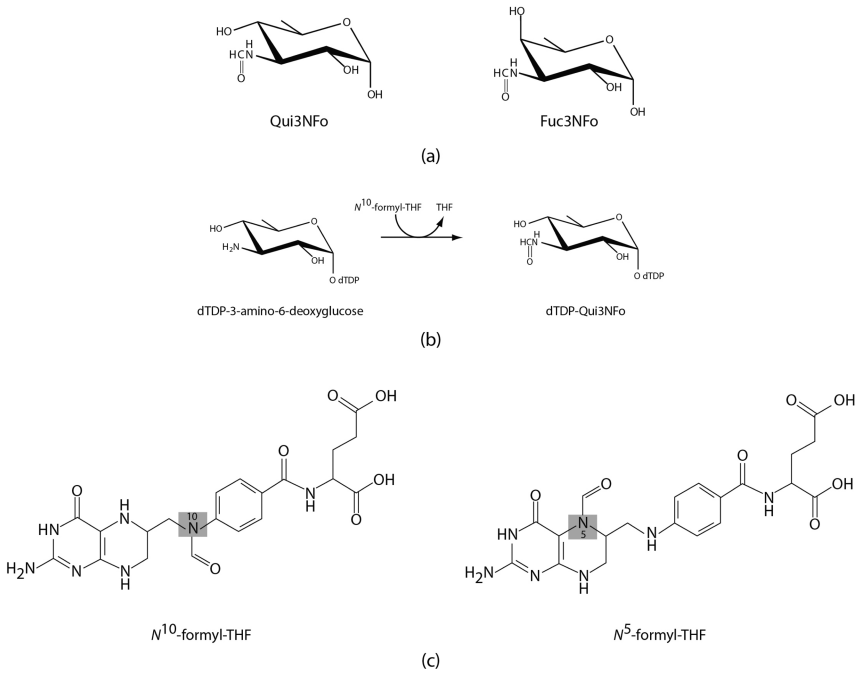

MATERIALS AND METHODS

Protein Constructs, Expression, and Purification. The gene encoding QdtF from *P. alcalifaciens* serogroup O40 was synthesized by DNA2.0 with optimized *Escherichia coli* codon usage. An N-terminal tag of the sequence MGSSHHHHHH-SSENLYFQGA was included before the initial methionine residue, and this construct was placed into the pJ411 vector for protein expression. Details concerning protein purification are provided in the Supporting Information. The protein was dialyzed against 10 mM Tris-HCl (pH 8.0) and 200 mM NaCl and concentrated to 8−12 mg/mL on the basis of an extinction coefficient of 0.87 $(mg/mL)^{-1}$ cm^{-1} as calculated with DNASTAR.

Table 1. Kinetic Parameters

enzyme	K_m (mM)	k_{cat} (s^{-1})	k_{cat}/K_m (M^{-1} s^{-1})
wild-type with dTDP-Qui3N	0.45 ± 0.09	2.43 ± 0.31	5.4×10^3
W305A variant with dTDP-Qui3N	2.15 ± 0.35	1.75 ± 0.15	8.0×10^2
wild-type with dTDP-Fuc3N	4.18 ± 0.43	1.50 ± 0.21	3.6×10^2
W305A variant with dTDP-Fuc3N	5.52 ± 0.72	1.82 ± 0.32	3.3×10^2

Crystallization of QdtF. Prior to crystallization trials, the protein was incubated with 5 mM dTDP and 5 mM N^5-formyltetrahydrofolate (N^5-formyl-THF). Crystallization conditions were then surveyed by the hanging drop method of vapor diffusion using a sparse matrix screen developed in the laboratory. Single crystals of QdtF were grown by hanging drop diffusion against a precipitant solution containing 100 mM HEPPS (pH 8.0), 200 mM KCl, and 5−7% poly(ethylene glycol) 8000. The crystals belonged to space group $P4_12_12$ with the following unit cell dimensions: $a = b = 78.3$ Å, and $c = 151.1$ Å. The asymmetric unit contained one subunit.

The dTDP-sugar complexes were obtained by soaking the crystals in a solution composed of 100 mM HEPPS (pH 8.0), 15% poly(ethylene glycol) 8000, 200 mM KCl, 200 mM NaCl, 5 mM N^5-formyl-THF, and either 10 mM dTDP-Qui3N or 10 mM dTDP-Fuc3N. The solution was exchanged three or four times to ensure the removal of dTDP. The dTDP-Qui3N or dTDP-Fuc3N substrates were prepared as described in the Supporting Information.

Site-Directed Mutagenesis and Crystallization. The site-directed mutant protein, W305A, was generated via the QuikChange method of Stratagene. The protein variant was expressed and purified as described for the wild-type enzyme. Crystals were grown and soaked under conditions similar to those used for the wild-type enzyme.

Structural Analysis of QdtF. Prior to X-ray data collection, the crystals of the wild-type enzyme/dTDP-Qui3N/N^5-formyl-THF complex were transferred to a cryoprotectant solution containing 100 mM HEPPS (pH 8.0), 25% poly(ethylene glycol) 8000, 18% ethylene glycol, 300 mM KCl, 300 mM NaCl, 5 mM N^5-formyl-THF, and 10 mM dTDP-Qui3N. X-ray data were collected at 100 K with a Bruker AXS Platinum 135 CCD detector controlled by the Proteum software suite (Bruker AXS Inc.). The X-ray source was Cu Kα radiation from a Rigaku RU200 X-ray generator equipped with Montel optics and operated at 50 kV and 90 mA. These X-ray data were processed with SAINT version 7.06A (Bruker AXS Inc.) and internally scaled with SADABS version 2005/1 (Bruker AXS Inc.). Relevant X-ray data collection statistics are listed in Table S1 of the Supporting Information. The structure was determined via molecular replacement with the software package PHASER using as a search model the coordinates for another sugar *N*-formyltransferase determined in the laboratory (Protein Data Bank entry 4LXQ).[7,8] Iterative cycles of model building with COOT and refinement with REFMAC reduced R_{work} and R_{free} to 18.5 and 21.5%, respectively, from 30 to 1.5 Å resolution.[9,10] X-ray data from the wild-type enzyme/dTDP-Fuc3N/N^5-formyl-THF complex crystals were collected and

DOI: 10.1021/bi501539a
Biochemistry 2015, 54, 631−638

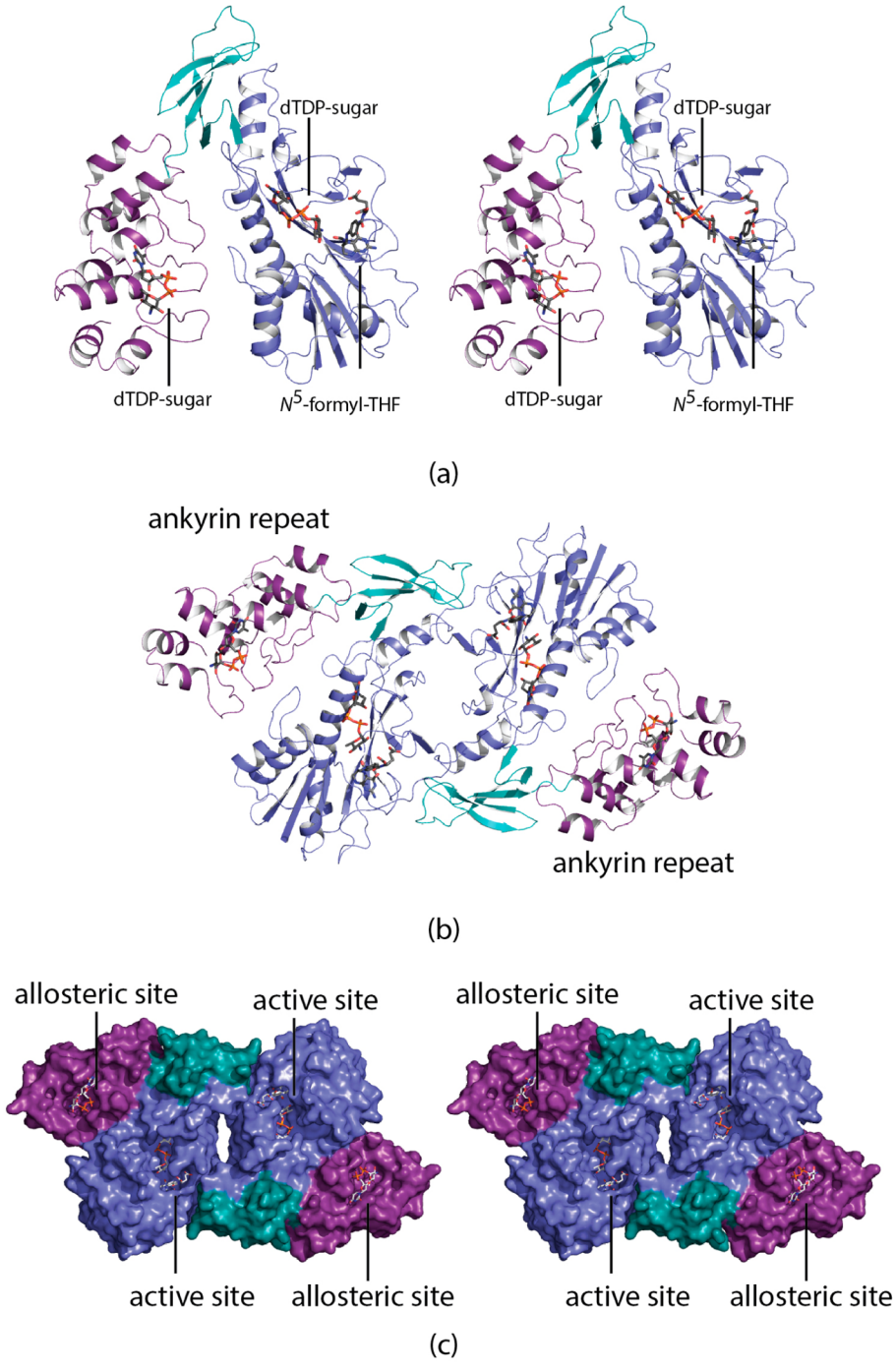

Figure 1. Overall structure of QdtF. The enzyme crystallized in space group $P4_12_12$ with one subunit in the asymmetric unit. A ribbon representation of the subunit is displayed in stereo in panel a. The N-terminal, middle, and C-terminal domains are colored blue, cyan, and purple, respectively. The dTDP-sugar ligands and the N^5-formyl-THF cofactor are depicted as sticks. The quaternary structure of QdtF is dimeric as shown in panel b. A surface representation of the dimer is depicted in stereo in panel c. Note that both the active site and the allosteric binding pocket are quite shallow and solvent-exposed.

processed in a similar manner. This complex structure was determined via difference Fourier methods. Iterative cycles of model building with COOT and refinement with REFMAC reduced R_{work} and R_{free} to 20.7 and 26.5%, respectively, from 30 to 1.8 Å resolution.

Crystals of the W305A variant with dTDP-Qui3N and N^5-formyl-THF were prepared and X-ray data collected in a manner similar to that described above. Relevant X-ray data collection statistics are listed in Table S1 of the Supporting Information. Iterative cycles of model building with COOT and refinement with REFMAC reduced R_{work} and R_{free} to 18.1 and 20.8%, respectively, from 30 to 1.50 Å resolution.[9,10] Model refinement statistics for all three protein complexes are listed in Table S2 of the Supporting Information.

Kinetic Analysis. In general, the kinetic constants for wild-type QdtF with its natural substrate dTDP-Qui3N or with the alternative substrate dTDP-Fuc3N or the W305A variant of QdtF with dTDP-Qui3N or dTDP-Fuc3N were determined via

DOI: 10.1021/bi501539a
Biochemistry 2015, 54, 631−638

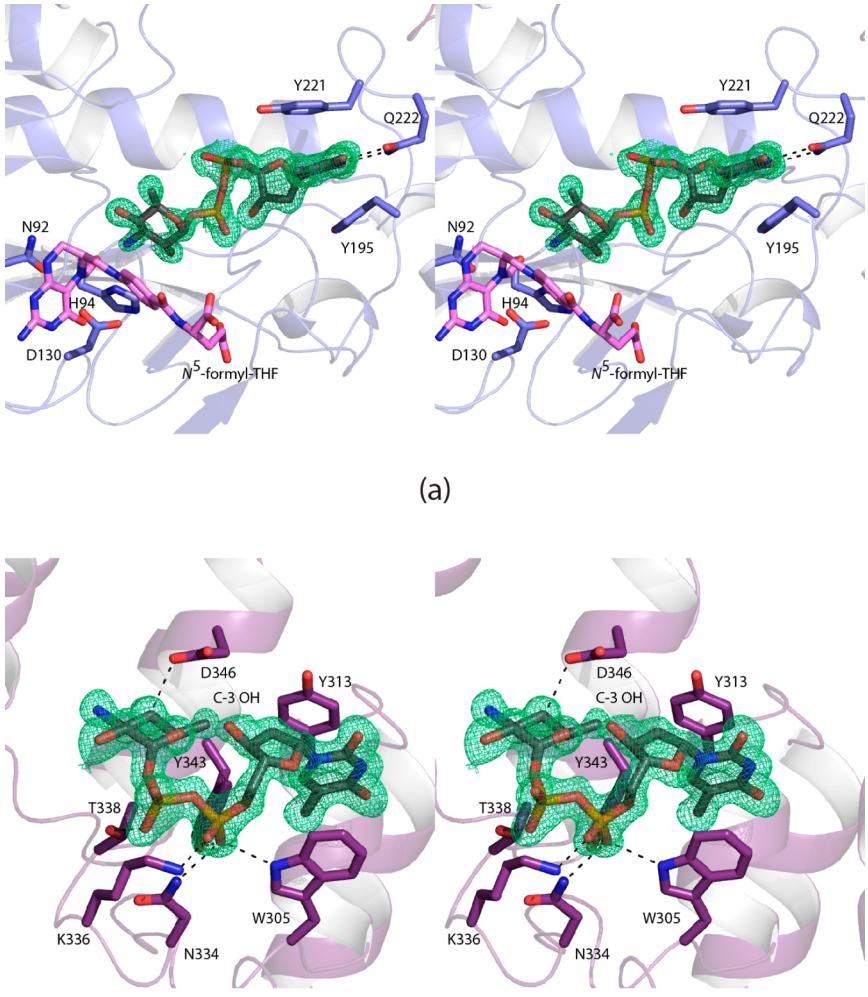

Figure 2. Observed electron density for the bound dTDP-sugar ligands. The electron density corresponding to the dTDP-sugar bound in the active site is displayed in panel a. The map, contoured at 3σ, was calculated with coefficients of the form $F_o - F_c$, where F_o is the native structure factor amplitude and F_c the calculated structure factor amplitude. The electron density corresponding to the dTDP-sugar bound in the allosteric binding pocket is shown in panel b. The map was calculated and contoured as described for panel a. Interactions (<3.2 Å) between the dTDP-sugars and the protein side chains are indicated by the dashed lines.

a discontinuous assay using an ÄKTA HPLC system. The reaction rates were determined by calculating the amount of formylated product (dTDP-Qui3NFo or dTDP-Fuc3NFo) produced on the basis of the peak area on the HPLC trace as measured at 267 nm. The area was correlated to concentration via a calibration curve created with standard samples that had been treated in the same manner as the reaction aliquots.

Specifically, the kinetic parameters for the wild-type enzyme with dTDP-Qui3N as a substrate were determined using 1 mL reaction mixtures containing 5 mM N^{10}-formyl-THF, 50 mM HEPPS (pH 8.0), 0.83 μM enzyme, and substrate concentrations ranging from 0.05 to 4.0 mM dTDP-Qui3N. Four 250 μL aliquots were taken at time points over 4 min and reactions quenched by the addition of 12 μL of 6 M HCL. Afterward, 200 μL of carbon tetrachloride was added, the samples were vigorously mixed and spun at 14000g for 1 min, and 200 μL of the aqueous phase was taken for subsequent analysis via HPLC. The samples were diluted with 2 mL of water and loaded onto a 1 mL ResQ column. The products were quantified after elution with an 8 column volume gradient from 0 to 400 mM LiCl (pH 4, HCl). The kinetic parameters of the wild-type enzyme with dTDP-Fuc3N as a substrate were determined in a similar manner using 1.25 μM enzyme and 0.5−20 mM dTDP-Fuc3N.

The kinetic parameters for the W305A variant with dTDP-Qui3N as a substrate were determined using 2.5 μM enzyme and 0.2−18 mM dTDP-Qui3N. Finally, the kinetic parameters for the W305A variant with dTDP-Fuc3N as a substrate were determined using 5.2 μM enzyme and 0.40−50.0 mM dTDP-Fuc3N. Plots of concentrations versus initial rates were analyzed using PRISM (GraphPad Software, Inc.) and fit to the equation $v_0 = (V_{max}[S])/(K_M + [S])$ for hyperbolic data and $v_0 = (V_{max}[S]^h)/(K_M{}^h + [S]^h)$ for sigmoidal data. Relevant kinetic parameters are listed in Table 1.

RESULTS AND DISCUSSION

The first structure of QdtF determined for this investigation utilized crystals of the enzyme in complex with its substrate, dTDP-3,6-dideoxy-3-amino-D-glucose (dTDP-Qui3N), and N^5-

DOI: 10.1021/bi501539a
Biochemistry 2015, 54, 631−638

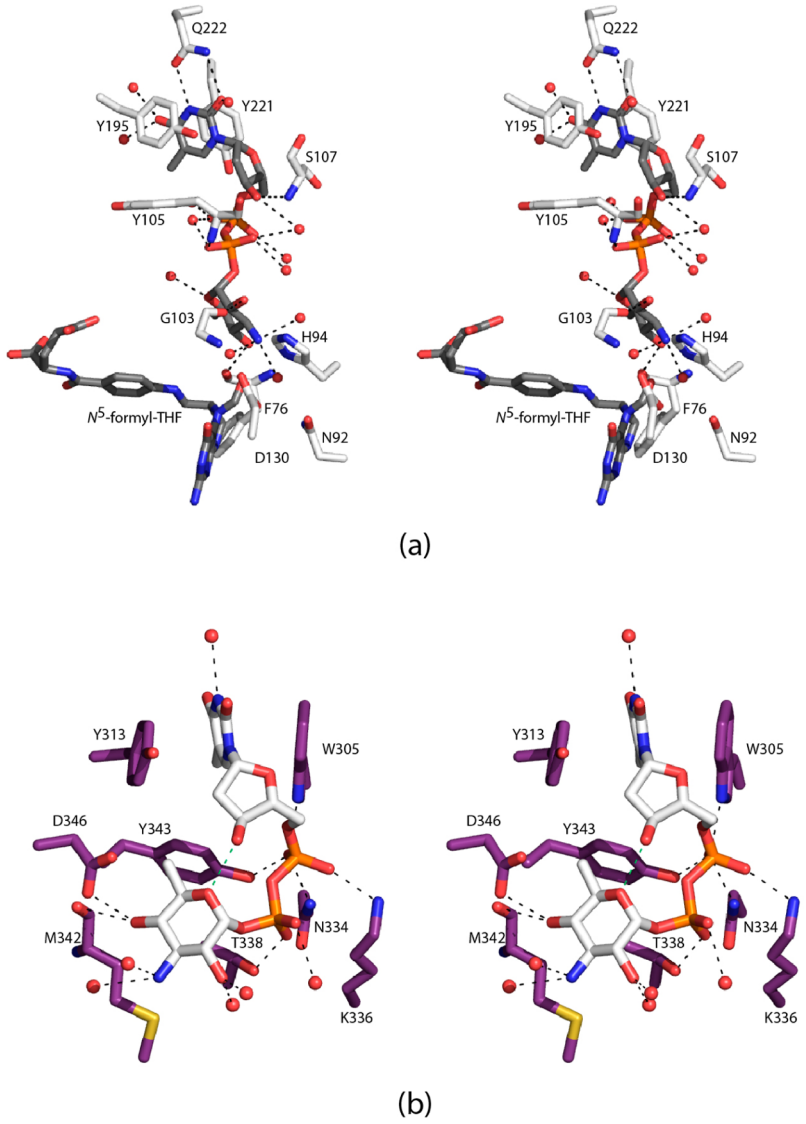

Figure 3. Close-up views of the active site and allosteric binding pocket. Shown in panel a is the active site region surrounding the dTDP-sugar substrate. Protein−ligand interactions of ≤3.2 Å are indicated by dashed lines. Ordered water molecules are depicted as red spheres. The dTDP-sugar substrate and N^5-formyl-THF are colored in gray bonds, whereas the protein bonds are displayed in white. Shown in panel b is the allosteric binding pocket with the protein side chains colored purple to emphasize that they belong to the ankyrin repeat domain. As in panel a, protein−ligand interactions of ≤3.2 Å are indicated by dashed lines, and ordered solvents are depicted as red spheres. The green dashed line indicates the presence of an intramolecular hydrogen bond in the dTDP-sugar substrate when it is bound in the allosteric binding pocket.

formyltetrahydrofolate (N^5-formyl-THF), a stable but catalytically inert cofactor. The model was refined to a nominal resolution of 1.5 Å ($R_{overall}$ = 18.5%, and R_{free} = 21.5%). Overall, the quality of the electron density was excellent such that it was possible to trace the entire polypeptide chain from Met 1 to Asn 397. The enzyme has one *cis* peptide linkage at Pro 99, which is located ∼14 Å from the active site. The histidine tag used for protein purification was not visible in the electron density map.

QdtF, like other sugar *N*-formyltransferases, functions as a dimer.[11,12] In the crystals utilized for this investigation ($P4_12_12$ space group), QdtF packed with its local 2-fold rotational axis coincident to the crystallographic dyad, thereby reducing the contents of the asymmetric unit to one subunit. A ribbon representation of the subunit is displayed in Figure 1a. As can be seen, it is composed of the three domains: the N-terminal region that is dominated by eight β-strands and six helices (Met 1−Leu 223), the middle motif that is composed of a β-hairpin and a four-stranded antiparallel β-sheet (Pro 224−Asn 271), and the C-terminal region, which contains ankyrin repeats (Phe 272−Asn 397). The ankyrin repeat itself is a helix−loop−helix motif composed of ∼33 amino acid residues with the α-helices running antiparallel and an extended loop at the C-terminus projecting outward at an ∼90° angle.[6] Most proteins with ankyrin motifs contain between four and seven repeats, but some, such as the cytoskeletal protein ankyrin, contain 24.[13,14] In the case of QdtF, there are three complete ankyrin repeats.

A ribbon representation of the QdtF dimer, with overall dimensions of ∼66 Å × 66 Å × 130 Å, is shown in Figure 1b. The total buried surface area at the dimer interface is ∼2100 Å^2. Notably, whereas the N-terminal and middle domains of each subunit provide side chains for the formation of the subunit−subunit interface, the ankyrin repeats splay away from the main body of the molecule. The N-terminal domain harbors the

DOI: 10.1021/bi501539a
Biochemistry 2015, 54, 631−638

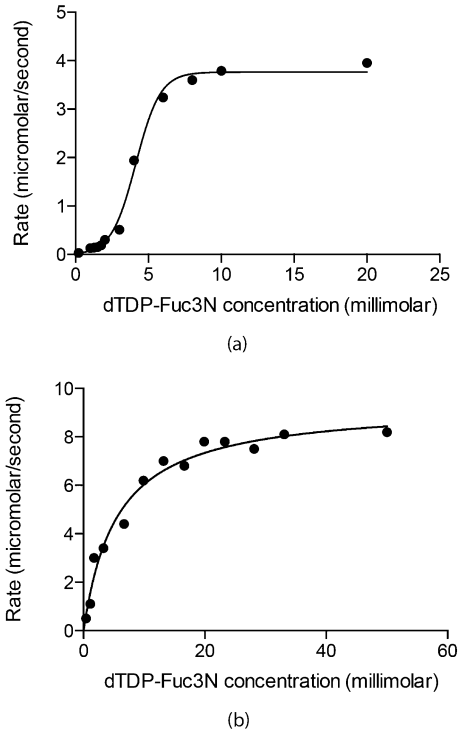

Figure 4. Kinetic behavior using dTDP-Fuc3N as a substrate. A plot of the reaction rate vs dTDP-Fuc3N concentration for the wild-type enzyme is shown in panel a. Panel b shows the plot for the W305A mutant protein.

active site cleft, which is shallow and solvent accessible (Figure 1c). The ankyrin repeat region provides a second shallow binding pocket for dTDP-3,6-dideoxy-3-amino-D-glucose. A distance of ~25 Å separates the two dTDP-sugar ligand binding pockets within the subunit.

Shown in panels a and b of Figure 2 are the electron densities corresponding to the two dTDP-sugar ligands observed binding to the QdtF subunit. The dTDP-Qui3N substrate adopts an extended conformation in the active site, whereas in the auxiliary binding pocket, it assumes a quite curved structure with the ribose C-3 hydroxyl oxygen lying within 3.0 Å of the hexose endocyclic oxygen. A close-up view of the QdtF active site is provided in Figure 3a. The thymine ring of dTDP-Qui3N is wedged between Tyr 195 and Tyr 221 and is hydrogen bonded to three water molecules and the carboxamide group of Gln 222. The backbone amide nitrogens of Tyr 105 and Ser 107 and the carbonyl oxygens of Phe 76 and Gly 103 provide additional protein–substrate interactions. Twelve water molecules surround the dTDP-Qui3N substrate. With the exception of Gln 222, however, there are no other side chains that directly interact with the dTDP-sugar. The positions of Asn 92, His 94, and Asp 130 are shown in Figure 3a because these residues are conserved among various *N*-formyltransferases, including WlaRD from *Campylobacter jejuni*,[11] ArnA from *E. coli*,[15] *E. coli* L-methionyl-tRNA *N*-formyltransferase,[16] and *E. coli* glycinamide ribonucleotide transformylase.[17] These amino acid residues have been implicated in catalysis. In the case of WlaRD, for example, the N94A, H96N, and D132N site-directed mutant proteins demonstrate no enzymatic activity under the assay conditions employed.[11]

A close-up view of the auxiliary binding pocket is shown in Figure 3b. In contrast to that observed in the active site, in the auxiliary binding pocket there are numerous interactions between the dTDP-sugar and the protein side chains. Specifically, Trp 305, Tyr 313, Asn 334, Lys 336, Thr 338, Tyr 343, and Asp 346 serve to anchor the dTDP-Qui3N ligand into the ankyrin repeat domain. To address the role of the auxiliary binding pocket in the catalytic activity of QdtF, a site-directed mutant protein, W305A, was subsequently prepared, its enzymatic activity measured, and its structure determined to 1.5 Å resolution in the presence of dTDP-Qui3N and N^5-formyl-THF ($R_{overall}$ = 18.1%, and R_{free} = 20.8%). It was reasoned that removal of the parallel stacking interaction between the indole ring of Trp 305 and the thymine ring of dTDP-Qui3N would abolish dTDP-sugar binding. Indeed, the electron density map showed no trace of dTDP-sugar binding in the second pocket, whereas the electron density corresponding to dTDP-Qui3N in the active site was unambiguous (Figure S1 of the Supporting Information). Importantly, the α-carbons for the wild-type enzyme and the W305A mutant protein superimpose with a root-mean-square deviation of 0.12 Å, thus indicating that removal of ligand binding to the site located in the ankyrin domain had little effect on the overall three-dimensional structure of QdtF. Ordered solvent molecules simply moved into the position vacated by the dTDP-Qui3N ligand.

As described in Materials and Methods, the catalytic activities of the wild-type enzyme and the W305A protein were investigated via an HPLC discontinuous assay. Plots of initial velocities versus dTDP-Qui3N concentrations for the wild-type enzyme and the W305A variant demonstrated Michaelis–Menten kinetics (Figure S2 of the Supporting Information). Relevant kinetic parameters are listed in Table 1. The catalytic efficiency of the W305A protein is reduced from 5400 to 800 M^{-1} s^{-1}. Whereas the k_{cat} values for the two proteins are similar within experimental error, removal of ligand binding from the auxiliary pocket increased the K_m for dTDP-Qui3N from 0.45 mM for the wild-type enzyme to 2.15 mM for the W305A variant. Clearly, the binding of a dTDP-sugar to the auxiliary pocket of QdtF plays a subtle yet measurable allosteric role. Whether the binding of the dTDP-sugar to the auxiliary pocket affects the rate of formation of the Michaelis complex or the rate of its dissociation to free enzyme and substrate is not known, however.

Given the observation that the active site region surrounding the C-4′ amino group of dTDP-Qui3N is relatively open, the activity of QdtF against dTDP-3,6-dideoxy-3-amino-D-galactose (dTDP-Fuc3N) was also tested. QdtF is, indeed, capable of turning over the alternative substrate albeit at a reduced catalytic efficiency of 360 M^{-1} s^{-1} (Table 1). Strikingly, an initial velocity plot using the wild-type enzyme against dTDP-Fuc3N concentration demonstrated sigmoidal kinetics (Figure 4a). The calculated Hill slope of 5.1 ± 0.6 indicates positive cooperativity. These data demonstrate that QdtF exhibits homotropic allostery with respect to the dTDP-Fuc3N substrate and thus has the proper architecture for communication between the active site and the auxiliary binding pocket. The identity of the ligand that regulates the activity of QdtF *in vivo* is not known at present. As a control, the catalytic activity of the W305A variant was also tested against the alternative substrate dTDP-Fuc3N. Hyperbolic kinetics were again observed as would be expected given the removal of ligand binding from the ankyrin domain (Table 1 and Figure 4b).

To complete the investigation of QdtF, we determined its structure in the presence of dTDP-Fuc3N and N^5-formyl-THF

DOI: 10.1021/bi501539a
Biochemistry 2015, 54, 631–638

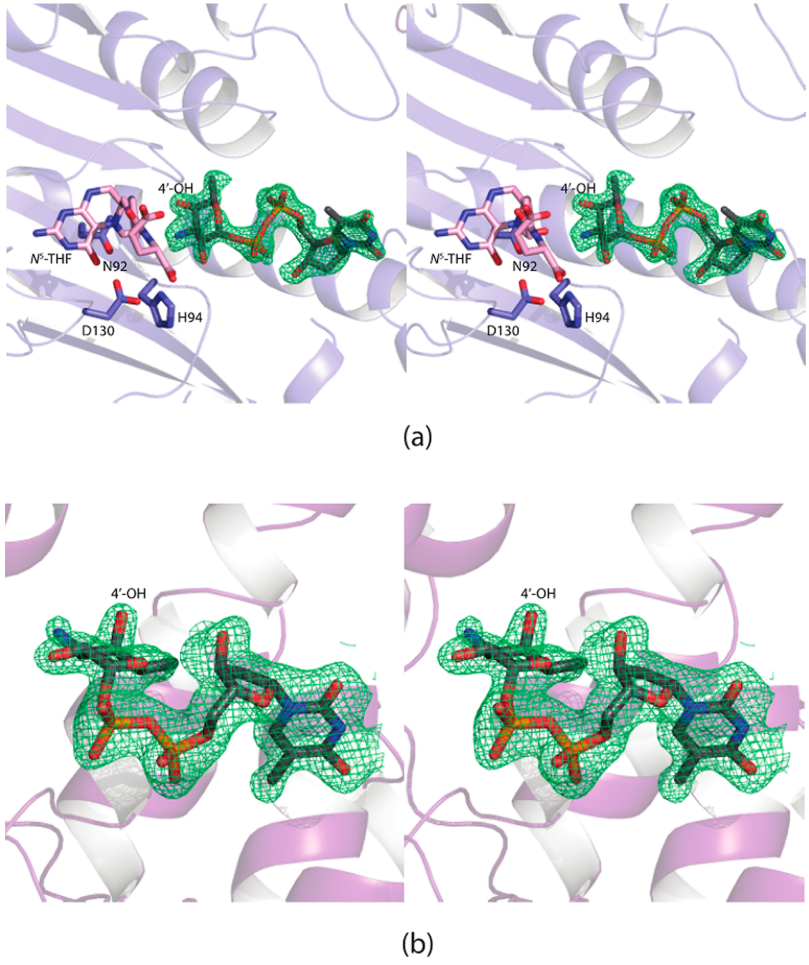

Figure 5. Electron density for the dTDP-Fuc3N ligand bound to wild-type QdtF. The observed electron density for the dTDP-Fuc3N ligand in the active site is shown in panel a. The map was calculated as described in the legend of Figure 2 and contoured at 3σ. The N^5-formyl-THF cofactor is highlighted in pink bonds. The observed electron density for the dTDP-Fuc3N sugar in the auxiliary binding site is displayed in panel b. The map was contoured at 3σ.

to 1.8 Å resolution. The electron densities corresponding to the dTDP-Fuc3N ligand in the active site and in the auxiliary binding pocket are shown in panels a and b of Figure 5, respectively. The α-carbons for the QdtF models with either bound dTDP-Qui3N or dTDP-Fuc3N superimpose with a root-mean-square deviation of 0.13 Å. The active site geometries of QdtF in the presence of either dTDP-Qui3N or dTDP-Fuc3N are nearly identical within experimental error. The C-3′ amino group is shifted by ∼0.4 Å in the active site. With respect to the allosteric pocket, the only major change occurs in the side chain conformation of Asp 346. When dTDP-Qui3N is bound, the carboxylate group of Asp 346 lies within hydrogen bonding distance of the C-4′ hydroxyl group of the pyranosyl ring (Figure 3b). In the presence of dTDP-Fuc3N, the side chain of Asp 346 swings out of the pocket.

The majority of ankyrin repeat proteins studied thus far have been isolated from eukaryotes, although it is becoming apparent from amino acid sequence analyses that the motif is also found in some bacterial and viral proteins.[4,14,18,19] Little is known, however, regarding the physiological roles of ankyrin repeats in prokaryotes. Their prevalence in proteins from intracellular pathogens such as *Legionella pneumophila* is especially intriguing, however.[20] A search of the QdtF sequence against the National Center for Biotechnology data bank shows that the enzyme is homologous to an additional eight putative *N*-formyltransferases that contain ankyrin repeats (Figure S3 of the Supporting Information). Importantly, Trp 305 and Tyr 313 in QdtF are completely conserved among these proteins, suggesting that the allosteric binding pocket is functional in these enzymes, as well. Many of these putative *N*-formyltransferases are found in pathogenic organisms such as *Pantoea stewartii*, which causes Stewart's wilt of sweet corn, *Francisella tularensis*, the causative agent of rabbit fever, and *Pseudomonas fuscovaginae*, which is responsible for brown sheath rot in rice. The discovery of an ankyrin repeat domain in QdtF that harbors an additional dTDP binding site was completely unexpected, and indeed, ankyrin repeats have never been implicated in small molecule binding. This study thus paves the way for new investigations focusing on the use of ankyrin repeats in allosteric regulation.

■ ASSOCIATED CONTENT

Supporting Information

Scheme S1, Figures S1−S3, and Tables S1 and S2. This material is available free of charge via the Internet at http://pubs.acs.org.

Accession Codes

Coordinates have been deposited in the Protein Data Bank (entries 4XCZ, 4XD0, and 4XD1).

DOI: 10.1021/bi501539a
Biochemistry 2015, 54, 631−638

AUTHOR INFORMATION

Corresponding Author

*E-mail: hazel_holden@biochem.wisc.edu. Fax: (608) 262-1319. Phone: (608) 262-4988.

Funding

Funding in part was from the National Institutes of Health (DK47814 to H.M.H.).

Notes

The authors declare no competing financial interest.

ACKNOWLEDGMENTS

We thank Professors Grover L. Waldrop and Gregory A. Grant for helpful discussions.

ABBREVIATIONS

dTDP, thymidine diphosphate; dTMP, thymidine monophosphate; HEPPS, *N*-(2-hydroxyethyl)piperazine-*N*′-3-propanesulfonic acid; HPLC, high-performance liquid chromatography; Tris, tris(hydroxymethyl)aminomethane.

REFERENCES

(1) Raetz, C. R., and Whitfield, C. (2002) Lipopolysaccharide endotoxins. *Annu. Rev. Biochem. 71*, 635−700.

(2) Murata, T., Iida, T., Shiomi, Y., Tagomori, K., Akeda, Y., Yanagihara, I., Mushiake, S., Ishiguro, F., and Honda, T. (2001) A large outbreak of foodborne infection attributed to *Providencia alcalifaciens*. *J. Infect. Dis. 184*, 1050−1055.

(3) Breeden, L., and Nasmyth, K. (1987) Similarity between cell-cycle genes of budding yeast and fission yeast and the Notch gene of *Drosophila*. *Nature 329*, 651−654.

(4) Bork, P. (1993) Hundreds of ankyrin-like repeats in functionally diverse proteins: Mobile modules that cross phyla horizontally? *Proteins 17*, 363−374.

(5) Mosavi, L. K., Cammett, T. J., Desrosiers, D. C., and Peng, Z. Y. (2004) The ankyrin repeat as molecular architecture for protein recognition. *Protein Sci. 13*, 1435−1448.

(6) Li, J., Mahajan, A., and Tsai, M. D. (2006) Ankyrin repeat: A unique motif mediating protein-protein interactions. *Biochemistry 45*, 15168−15178.

(7) McCoy, A. J., Grosse-Kunstleve, R. W., Adams, P. D., Winn, M. D., Storoni, L. C., and Read, R. J. (2007) Phaser crystallographic software. *J. Appl. Crystallogr. 40*, 658−674.

(8) Davis, M. L., Thoden, J. B., and Holden, H. M. (2007) The X-ray structure of dTDP-4-keto-6-deoxy-D-glucose-3,4-ketoisomerase. *J. Biol. Chem. 282*, 19227−19236.

(9) Emsley, P., and Cowtan, K. (2004) Coot: Model-building tools for molecular graphics. *Acta Crystallogr. D60*, 2126−2132.

(10) Murshudov, G. N., Vagin, A. A., and Dodson, E. J. (1997) Refinement of macromolecular structures by the maximum-likelihood method. *Acta Crystallogr. D53*, 240−255.

(11) Thoden, J. B., Goneau, M. F., Gilbert, M., and Holden, H. M. (2013) Structure of a sugar *N*-formyltransferase from *Campylobacter jejuni*. *Biochemistry 52*, 6114−6126.

(12) Zimmer, A. L., Thoden, J. B., and Holden, H. M. (2014) Three-dimensional structure of a sugar *N*-formyltransferase from *Francisella tularensis*. *Protein Sci. 23*, 273−283.

(13) Lux, S. E., John, K. M., and Bennett, V. (1990) Analysis of cDNA for human erythrocyte ankyrin indicates a repeated structure with homology to tissue-differentiation and cell-cycle control proteins. *Nature 344*, 36−42.

(14) Al-Khodor, S., Price, C. T., Kalia, A., and Abu Kwaik, Y. (2010) Functional diversity of ankyrin repeats in microbial proteins. *Trends Microbiol. 18*, 132−139.

(15) Williams, G. J., Breazeale, S. D., Raetz, C. R., and Naismith, J. H. (2005) Structure and function of both domains of ArnA, a dual function decarboxylase and a formyltransferase, involved in 4-amino-4-deoxy-L-arabinose biosynthesis. *J. Biol. Chem. 280*, 23000−23008.

(16) Schmitt, E., Blanquet, S., and Mechulam, Y. (1996) Structure of crystalline *Escherichia coli* methionyl-tRNA(f)Met formyltransferase: Comparison with glycinamide ribonucleotide formyltransferase. *EMBO J. 15*, 4749−4758.

(17) Almassy, R. J., Janson, C. A., Kan, C. C., and Hostomska, Z. (1992) Structures of apo and complexed *Escherichia coli* glycinamide ribonucleotide transformylase. *Proc. Natl. Acad. Sci. U.S.A. 89*, 6114−6118.

(18) Voth, D. E. (2011) ThANKs for the repeat: Intracellular pathogens exploit a common eukaryotic domain. *Cellular Logistics 1*, 128−132.

(19) Jernigan, K. K., and Bordenstein, S. R. (2014) Ankyrin domains across the tree of life. *PeerJ 2*, e264.

(20) Campanacci, V., Mukherjee, S., Roy, C. R., and Cherfils, J. (2013) Structure of the *Legionella* effector AnkX reveals the mechanism of phosphocholine transfer by the FIC domain. *EMBO J. 32*, 1469−1477.

DOI: 10.1021/bi501539a
Biochemistry 2015, 54, 631−638